

CNRS
Centre National de la Recherche Scientifique

INFN
Istituto Nazionale di Fisica Nucleare



Use of the photon calibrators for the VSR1 calibration

F. Marion, B. Mours, L. Rolland

VIR-053A-08

June 26, 2008

VIRGO * A joint CNRS-INFN Project
Project office: Traversa H di via Macerata - I-56021 S. Stefano a Macerata, Cascina (PI)
Secretariat: Telephone (39) 50 752 521 – Fax (39) 50 752 550 – e-mail virgo@pisa.infn.it

Contents

1	Introduction	2
2	Principle of the photon calibrator, mirror-induced movement	3
3	Photon calibrator setup during VS1	3
3.1	Location of the photon calibrators	3
3.2	Laser beam characteristics	5
3.3	View-ports transmission factors	5
4	Calibration of the NI photon calibrator	7
4.1	Measurements setup	7
4.1.1	Powermeter description	7
4.1.2	Measurements description	8
4.2	NI photon calibrator calibration	8
5	Mirror actuator calibration	12
5.1	Data configurations	12
5.2	Analysis method	12
5.2.1	Principle	12
5.2.2	Detailed computation	14
5.3	Results: mirror coil actuation gain	14
5.3.1	NI mirror coil actuation	15
5.3.2	NE mirror coil actuation	15
5.3.3	WE mirror coil actuation	15
6	Conclusions	21

1 Introduction

The aim of the photon calibration (pcal) is the validation as and independent check of the main stream mirror actuation calibration [1].

In this note, the pcal are used to check the calibration of the first Virgo scientific run VSR1 (May 18th to October 1st, 2007). The measurements were performed during post-VSR1 calibration, in November 2007.

The principle of the photon calibration is first given. The pcal setup is then described. Direct measurements of the mirror actuation modulus can be estimated using the pcal. They are detailed and the results are compared to the main stream calibration results.

The pcal can also be used as a global check of the h-reconstruction. This will be described in another note, specific to the h-reconstruction checks.

2 Principle of the photon calibrator, mirror-induced movement

A photon calibrator consists in an auxiliary laser hitting an arm mirror of the Virgo interferometer (ITF). The pressure of the laser radiation on the mirror induces a movement of the suspended mirror. Knowing the induced mirror movement is the key of all the following analysis in order to calibrate the mirror coil actuations.

The force induced by the pcal laser beam on the ITF mirror is perpendicular to the mirror surface. It is given by¹:

$$F(t) = \frac{2 \cos i}{c} \mathcal{P}(t) \quad (1)$$

where $\mathcal{P}(t)$ is the power reflected by the mirror as function of time, i is the incidence angle of the laser beam on the ITF mirror and c is the light speed.

The mirror of mass m is suspended to the pendulum with resonance frequency of the order of 0.6 Hz. The amplitude of its longitudinal movement at frequencies larger than ~ 50 Hz, is given as function of the amplitude F_0 of the laser pressure force:

$$\Delta L_{pcal}(f) \sim \frac{F_0(f)}{m \times \omega^2} = \frac{2 \cos i}{c} \mathcal{P}_0(f) \frac{1}{m \times (2\pi f)^2} \quad (2)$$

where \mathcal{P}_0 is the amplitude of the laser power reflected by the mirror.

3 Photon calibrator setup during VS1

The setup of the pcal used for the calibration of VSR1 is described in this section.

3.1 Location of the photon calibrators

The location of the optical benches on the NI and WI towers are shown in the figure 1. The viewports are identified with 3 coordinates: position side, corner, vertical position (up or down). For the NI pcal, the laser is injected through the viewport (N,W,U), the reflected and transmitted beams are seen through the viewports (N,E,D) and (S,E,D) respectively. For the WI pcal, the laser is injected through the viewport (W,S,U), the reflected and transmitted beams are seen through the viewports (W,N,D) and (E,N,D) respectively. The viewports have a diameter of 138 mm.

The setup of the injection benches is given in the figure 2. The optical bench is a 30 cm \times 30 cm table. The laser beam is collimated. A large fraction of the beam ($\sim 99\%$) is reflected on the

¹ For a single photon of energy $h\nu$, the variation of momentum of a free mirror of mass m is given by $dp = m \cdot dv = 2 \frac{h\nu}{c} \cos i$.

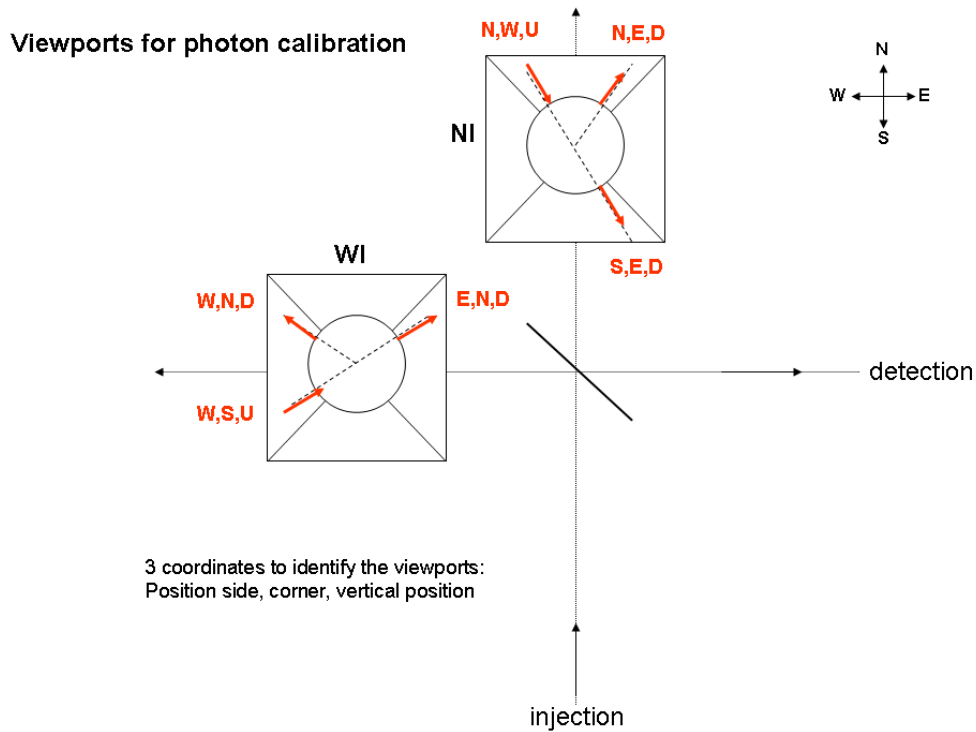


Figure 1: *Location of the pcal optical benches.* The viewports are identified with 3 coordinates: position side, corner, vertical position (up or down).

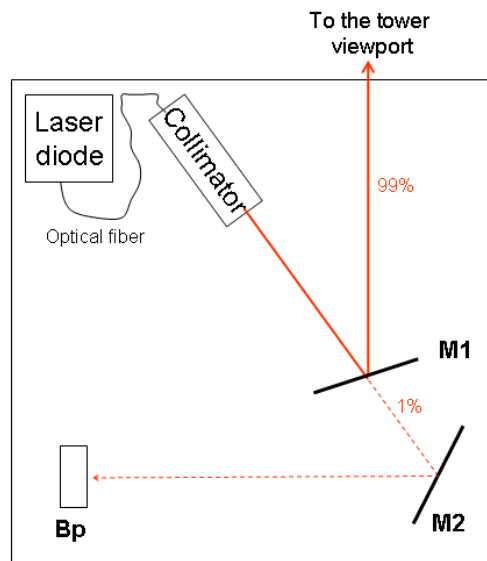


Figure 2: *Optical setup of the pcal injection bench.*

mirror M1 to the input tower mirror. A small fraction is transmitted to the mirror M2 which focalize the beam onto the photodiode Bp. The photodiode is used to monitor the power of the pcal laser beam. It is read and stored in the DAQ in the channel *Ca_NI_ADC* (*Ca_WI_ADC*). The characteristics of the mirrors are given in the table 1.

The optical bench is set to form an angle of 16° with the horizontal plane. With such an angle, a beam emitted at 10 cm above and parallel to the bench level crosses the plane containing the horizontal axe of the input mirror. The incident angle of the pcal laser beam and the input mirror axe has been estimated [2] to 40° . The uncertainty on this angle is estimated to 1° .

	M1	M2
Reflectivity	$(99 \pm 1) \%$	$(99.5 \pm 0.1) \%$
Transmitivity	$(0.9 \pm 0.1) \%$	-
Focal length (mm)	flat	200

Table 1: **Pcal mirror characteristics.** The intensity reflection and transmission factors are given as well as the focal length of the mirrors.

Nothing is installed on the output benches where the reflected and injected beams arrive. Manual power measurements are performed to calibrate the pcal (see section 4).

3.2 Laser beam characteristics

The laser diode has a wavelength of 915 nm and a maximum power of 1.2 W.

After collimation, the size of the pcal beam evolves with the propagated distance approximately as an exponential [2]. Its diameter can be approximated by:

$$d = A \times e^{-\frac{x}{x_0}} \quad (3)$$

with $A = 24$ and $x_0 = 1050$. The beam diameter is thus estimated to ~ 24 mm at the collimator output and to ~ 6 mm on the input mirror (at ~ 1.3 m).

3.3 View-ports transmission factors

The knowledge of the transmission factors of the different view ports of the pcal setup is important in order to estimate the laser power reflected by the main ITF mirror from power measurements made outside the tower.

They have been measured in 1987 from 480 to 900 nm while the laser beam has a wavelength of 915 nm. The measurements were performed with an incidence angle of the beam onto the view ports of 10° which is of the order of the present setup. The measurements have thus been extrapolated up to 915 nm. Thus, the numbers given in the table 2 have large systematic errors.

Tower id	Input view port	Reflected view port	Transmitted view port
NI	0.84%	0.84%	1.05%
WI	?%	?%	?%

Table 2: *Extrapolated intensity reflectivity coefficients of the pcal view ports at 915 nm. Measurements performed in 1987 with an incidence angle of 10° for wavelengths between 480 and 900 nm have been extrapolated up to 915 nm.*

4 Calibration of the NI photon calibrator

A precise calibration of the power reflected by the ITF mirror is needed in order to compute the mirror motion from equation 2. The pcal calibration consists in measuring the reflected laser power (in W) as function of the photodiode output (in V).

One advantage of the current setup is the possibility to measure the laser power of the three main beams at the same time as the photodiode output:

- the injected laser power (before the viewport)
- the reflected laser power (after the viewport)
- the transmitted laser power (after the viewport)

This allows to measure the power losses of the system which are taken into account as systematic errors.

4.1 Measurements setup

4.1.1 Powermeter description

The pcal laser power is measured using a powermeter *FieldMate* from Coherent. The accuracy of the digital meter is $\pm 1\%$.

The sensor is an *OP-2 IR* Germanium optical sensor. Its characteristics are given in the following table:

Name	OP-2 IR
Wavelength range (nm)	800-1800
Active area diameter (mm)	5
Maximum power (mW)	10
Power resolution (nW)	1
Calibration uncertainty (%)	4.5
Maximum average power density (W/cm ²)	0.5
Dimensions (mm)	∅ 29 × 19
Description	Germanium
RoHS compliant	Yes
Part number	1098416



The powermeter and the sensor have been bought in March 2007. Its calibration was done on March 2007 by the company.

The final error on the power measurements due to the powermeter accuracy and sensor calibration are thus estimated to be $\pm 5.5\%$.

4.1.2 Measurements description

The pcal laser power was controlled manually through its power supply. Different continuous powers were set to get different measurements. For every laser power, different measurements were performed:

- the injected laser power (before the viewport)
- the reflected laser power (after the viewport)
- the transmitted laser power (after the viewport)
- the photodiode output voltage. It was read using the dataDisplay tool online in order to include all the readout electronics and DAQ response as for the stored data.

Since the pcal laser beam size is larger than the powermeter head, a diaphragm is set at the output of the collimator. After clipping, the input beam visible size (as seen on a IR-optical conversion screen) is of the order of 1-2 mm. However, even with such a beam size the power measurements were very sensitive to the head position, indicating that the beam size was close to the head size.

An additionnal lens was used to focalise the beam on the powermeter head with a size lower than 1 mm. With such a configuration, the sensor could be displaced by a few mm keeping the same power measurement, and thus reducing the systematic errors. However, the transmittivity of the lens is unknown and add systematic errors on the measured powers.

4.2 NI photon calibrator calibration

The different measurements made on the NI pcal are given in the table 3. The use of the diaphragm limits the measurements to low laser power of the order of 50 mW.

In the following, errors of the measurements have been estimated to 0.6 mV on the photodiode readout and 3% on the laser power (an error of 0.1 mW is assumed in the dark). Such errors are still quite arbitrary and will need to be refined.

The data with such errors are shown on the figure 3. The photodiode readout response is linear as function of the input, reflected and transmitted laser powers. The availability of the three measurements allows to estimate the power losses in the calibration system. The third plot shows the ratio of the output power over the input power. Its average value is $91\% \pm 2\%$. The 9% power loss can be attributed to different origins:

- reflectivity of the three view ports of the tower (see table 2),
- absorption in the view ports and in the ITF mirror,
- systematic errors on the laser power measurements.

The last plot of the figure 3 shows the output to input power ratio *inside* the tower, after the correction of the losses due to the view port extrapolated reflectivities. There is still $7.3\% \pm 3.2\%$ power losses. This will be taken into account as systematic error since the location of the losses (before of after the reflection on ITF mirror) is unknown.

The power that needs to be calibrated as function of the photodiode readout is the power reflected by the ITF mirror. It can be estimated using two independent models:

- model 1 (P_{r1}^{NI}): the measured reflected power is corrected for the view port reflectivity (0.84%),
- model 2 (P_{r2}^{NI}): the measured input power is corrected for the input view port reflectivity (0.84%) and the ITF mirror reflectivity ($\sim 90\%$)

In order to reduce the systematic errors, a third model (P_{r3}^{NI}) was build averaging the former ones.

The figure 4 gives the reflected power on the NI mirror as function of the photodiode readout for the two models and the average. The average model will be used as the reference model to estimate the mirror movement as function of the photodiode readout in the calibration data. The reflected power on the NI mirror is estimated as function of the photodiode readout Ca_NI_ADC (in V):

$$P_{r3}^{\text{NI}} = p_0^{\text{NI}} + p_1^{\text{NI}} \times \text{Ca_NI_ADC} \quad (4)$$

$$P_{r3}^{\text{NI}} = (0.00487 \pm 0.00010) + (0.664 \pm 0.012) \times \text{Ca_NI_ADC} \quad (5)$$

The plot on the right shows the relative difference between the two models as function of the photodiode readout:

$$\frac{P_{r2}^{\text{NI}} - P_{r1}^{\text{NI}}}{P_{r2}^{\text{NI}}}$$

The average difference is $5\% \pm 4\%$, mainly due to the point measured at low power.

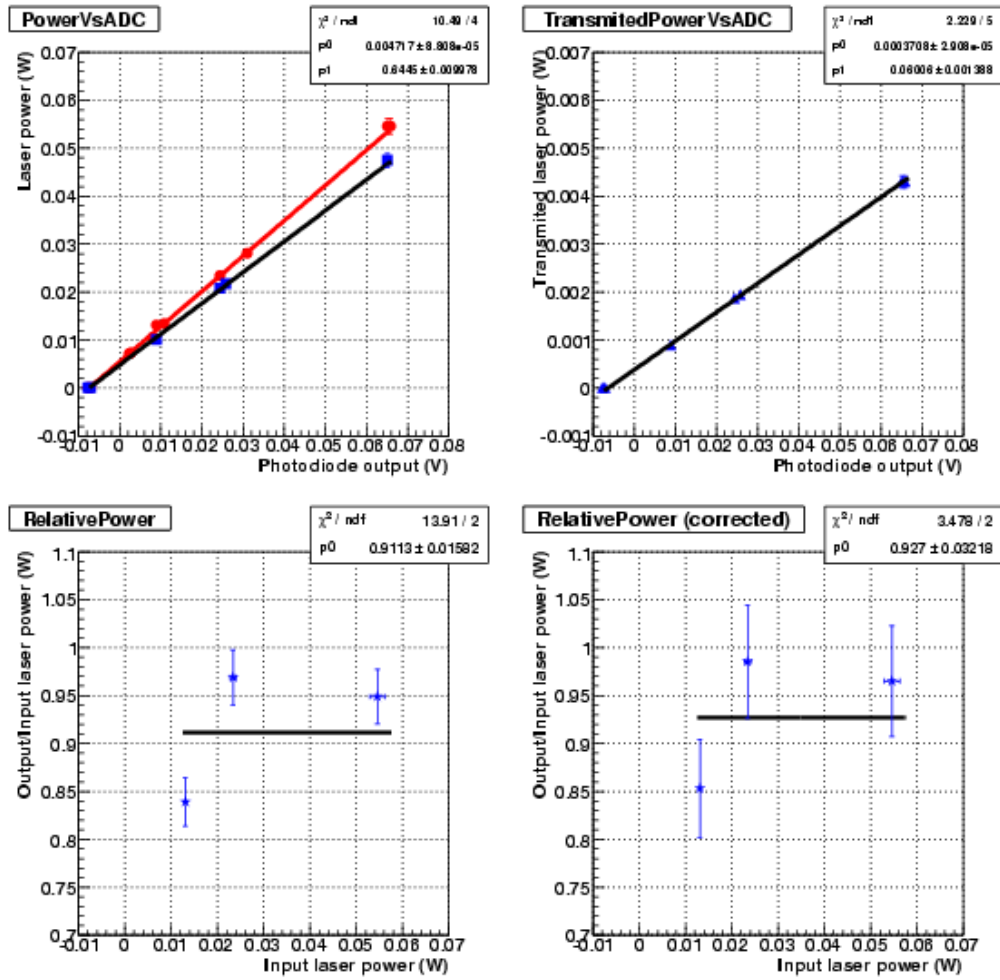


Figure 3: *Calibration of the NI pcal. Pad 1: measured input (red) and reflected (blue) laser power as function of the photodiode readout. Pad 2: measured transmitted laser power as function of the photodiode readout. Pad 3: ratio of the measured output power (reflected + transmitted) over the input power, as function of the input power. Pad 4: ratio of the output power (reflected + transmitted) over the input power, corrected for the view port transmission coefficients, as function of the measured input power.*

Ca_NI_ADC (mV)	Input power (mW)	Transmitted power (mW)	Reflected power (mW)
9.0	13.1	0.890	10.1
25.8	-	1.94	21.7
24.4	23.4	1.87	20.8
-7.035	0.0	0.0	0.0
-7.64	0.0	0.0	0.0
65.1	54.6	4.3	47.5
65.9	54.6	4.3	-
10.8	13.4	-	-
8.1	10.5	-	-
2.8	7.3	-	-
2.3	7.1	-	-
31.0	28.1	-	-

Table 3: *Measurements for the NI pcal calibration.*

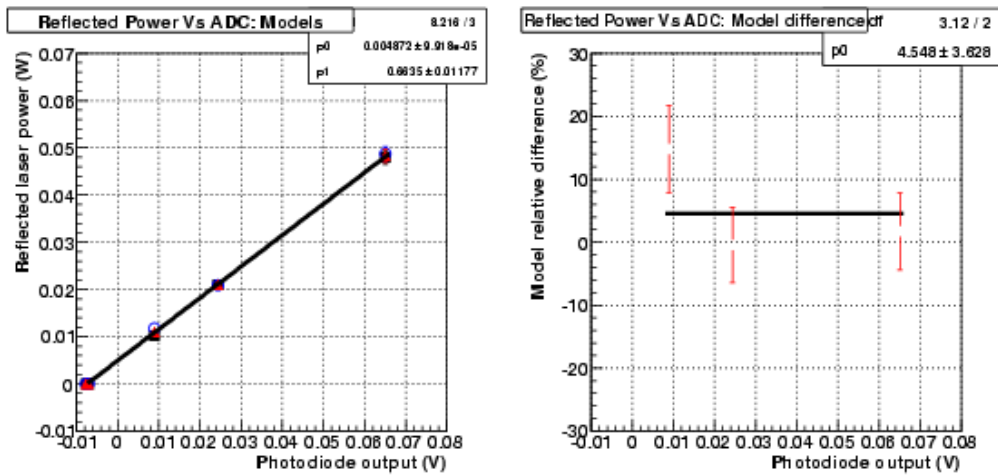


Figure 4: *Calibration of the NI pcal reflected beam power. Pad 1: reflected power computed with the the three models discussed in the text as function of the photodiode readout (black: model1, blue: model2, red: average) Pad 2: relative difference of the models 1 and 2 as function of the photodiode readout.*

5 Mirror actuator calibration

The photon calibrators can be used to measure the modulus of the mirror coil actuation transfer function (TF). This method is fully independent of the main stream calibration (including of the free swinging Michelson measurements).

The comparison of both results is an important check of the main stream calibration.

The mirror coil actuation TF modulus $A(f)$ is defined as the TF from the longitudinal control signal (i.e. Sc_NE_zCorr) to the mirror induced motion, corrected for the pendulum mechanical response $P(f)$ modelised as a second order low-pass filter with a gain of 1, a resonance frequency $f_{cut} = 0.6$ Hz and a quality factor $Q = 1000$.

5.1 Data configurations

The ITF is locked in step 12 with the suspensions in Low Noise (LN) mode. The input mirrors are driven simultaneously through the coil actuation and the pcal actuation. The end mirrors are driven through the coil actuation only.

The figure 5 describes the control-loop of the ITF mirror longitudinal movements. The dark fringe signal (channel Pr_B1_ACp) is noted as S . The different parts of the controls are:

- G : the actuation TF (m/V). It includes the actuation electronic TF A and the pendulum mechanical response P : $G = A \times P$.
- C : it includes the optical response of the ITF and the dark fringe sensing electronics.
- H : “global control” response.

Lines are injected on the mirror through the different paths:

- through the mirror actuators (all mirrors) at f_i . The injected lines f_i are computed by a CaRT server and sent to the mirror actuation DSP at the level of $Sc_ \{NE, NI, WE, WI\} _ LoopIn$.
- through the photon calibrator (input mirrors) at F_i . The laser power is measured by the pcal photodiode and sent to the channel $Ca_ \{NI, WI\} _ ADC$. The induced mirror movement ΔL_{pcal} of the lines F_i is directly computed from the calibrated laser power (see section 4).

The f_i and F_i frequencies are closed separated frequencies, offset by a few Hz (<2 Hz).

5.2 Analysis method

5.2.1 Principle

From the loop described in the figure 5, the dark fringe amplitudes can be estimated as function of the $LoopIn$ and the ΔL_{pcal} amplitudes, assuming that the injected noises dominate the loop

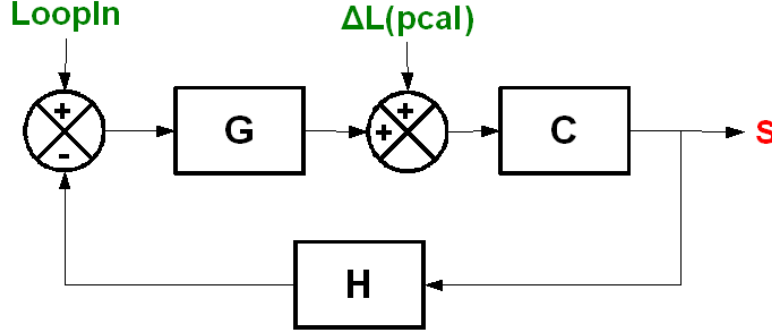


Figure 5: **Control loop of the ITF with the injections.** The location of the line injections to the mirror are shown.

at the injected frequencies:

$$S(f_i) = P(f_i) \times A(f_i) \times LoopIn(f_i) \times \frac{C(f_i)}{1 - C(f_i) \times P(f_i) \times A(f_i) \times H(f_i)} \quad (6)$$

$$S(F_i) = \Delta L_{pcal}(F_i) \times \frac{C(F_i)}{1 - C(F_i) \times P(F_i) \times A(F_i) \times H(F_i)} \quad (7)$$

The global Virgo TF in m/W is generally described as $V = \frac{1-C.P.A.H}{C}$. The mirror coil actuation gain is thus given by:

$$A(f_i) = \frac{S(f_i)}{S(F_i)} \frac{\Delta L_{pcal}(F_i)}{P(f_i) \times LoopIn(f_i)} \frac{V(f_i)}{V(F_i)} \quad (8)$$

$$A(f_i) = \frac{S(f_i)}{S(F_i)} \frac{Ca_NI_ADC(F_i) \times p_1 \times \alpha(F_i)}{P(f_i) \times LoopIn(f_i)} \frac{V(f_i)}{V(F_i)} \quad (9)$$

$$\text{where } \alpha(F_i) = \frac{2 \cos i}{c} \frac{1}{m(2\pi F_i)^2} \quad (\text{see equation 2}) \quad (10)$$

$$\text{and } p_1 \text{ is given in equation 5} \quad (11)$$

The photodiode readout signal $Ca_NI_ADC(F_i)$ is scaled by p_1 to get the laser power amplitude² $\mathcal{P}(F_i)$ and then by $\alpha(F_i)$ to get the mirror motion amplitude $\Delta L_{pcal}(F_i)$.

The figure 6 shows the ratio of the Virgo TF $\frac{V(f_i)}{V(F_i)}$ for closely separated frequencies on November 15th 2007. The ratio cannot be neglected. Below ~ 50 Hz, the ratio vary quicly with the frequency. Slight modifications of the Virgo TF might change the ratio by a large amount. Since the Virgo TF was not measured at the same time as the pcal injections, the pcal calibration might not be valid below 50 Hz.

Assuming that the ITF loops on the longitudinal motion of the mirrors react the same for the different mirrors, one can compute the coil actuation gain of any mirror using its *LoopIn* signal in the previous equation.

² $FFT[p_0 + p_1 \times V(t)](f) = p_1 \times FFT[V(t)](f)$ for $f \neq 0$.

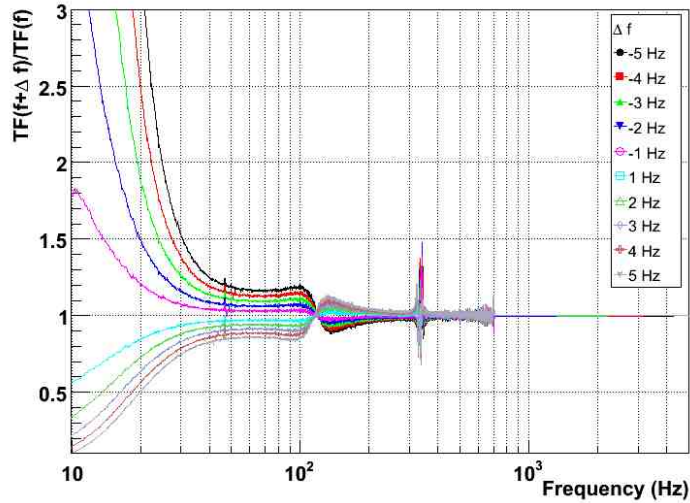


Figure 6: **Ratio** $\frac{V(f+\Delta f)}{V(f)}$ **of the Virgo TF** for Δf values between -5 and $+5$ Hz. The TF was measured on November 15th 2007 (GPS 879168508).

5.2.2 Detailed computation

Different TFs are computed according to the equation 9. The TFs of the dark fringe S to the injected noise are calculated, in W/V:

$$T_{coil}(f_i) = \frac{S(f_i)}{LoopIn(f_i)} \quad \text{and} \quad T_{pcal}(F_i) = \frac{S(F_i)}{Ca_NI_ADC(F_i)}$$

The mirror coil actuator TF modulus is then estimated in m/V as:

$$A(f_i) = \frac{1}{P(f_i)} \frac{T_{coil}(f_i)}{T_{pcal}(F_i) \frac{1}{p_1 \times \alpha}} \frac{V(f_i)}{V(F_i)} \quad (12)$$

A statistical error can be estimated for all the measured TFs that appear in this equation. The statistical error on p_1 is derived from the pcal absolute calibration. In the current analysis, the statistical error on α is assumed to be 0. The statistical error of $G(f_i)$ can thus be calculated from these measurements.

5.3 Results: mirror coil actuation gain

The mirror coil actuation gain as function of frequency has been measured for the arm mirrors using the NI pcal as described above. The suspensions were set in LN mode. The results are given in this section. They are then compared to the coil actuation gain measured with the main stream of the calibration and given in the note [1].

5.3.1 NI mirror coil actuation

The coil actuation gain of the NI mirror measured using the NI pcal are given in the table 4 for every datasets. The pcal lines below 450 Hz are injected altogether while the other lines are injected one by one. A set of ~ 20 lines was injected on the coil actuation permanently.

The pcal and coil lines (F_i and f_i) that were used to compute the gain are both given. The frequency offset is 1 Hz except for one of 4 Hz. The coherences of the dark fringe with the injected lines in *Ca_NI_ADC* and *Sc_NI_LoopIn* are higher than 95%. The statistical errors of a single measurement is of the order of 5%.

The points at 19 and 24 Hz are given for information but the model used to compute the pcal mirror motion is not valid below ~ 50 Hz as described above.

The data at a given frequencies have been averaged. The average coil actuation gain is given in the table 5 and in the figure 7.

Comparison with the main stream calibration results - The NI coil actuation in LN mode obtained by the main stream calibration are compared to the current results on the figure 7.

At low frequency (below a few 100's Hz), the mirror actuation gain estimated with the pcal are in agreement with the main stream calibration within 5%. Taking into account the systematic errors of the estimation with the pcal, of the order of 10-20%, this confirms that the main stream calibration is good within 10-20%.

At higher frequencies, the actuation gain estimated using the pcal is higher than the one from the main stream calibration. The effect is increasing with frequency, up to $\sim 40\%$ at 1 kHz. This effect has been observed by the GEO and LIGO collaborations and described in [3]. At high frequency, the mirror deformation induced by the radiation pressure of the pcal laser has an amplitude higher than the induced mirror motion. Since the pcal laser beam hits the center of the mirror, it is overlapped by the main ITF beam. The main beam thus "sees" the motion of the reflective surface which is the sum of the mirror motion and the mirror deformation. The difference between the pcal calibration and the main stream calibration at 1 kHz, expected from this effect, is of the order of 30-40%. The analysis described in this note is thus valid up to a few 100's Hz only, where the mirror deformation can be neglected.

5.3.2 NE mirror coil actuation

The same results as shown for the NI calibration are given in the table 6 and in the figure 8.

At low frequency, the calibration with the pcal is within $5\% \pm 10 - 20\%$ from the main stream calibration.

5.3.3 WE mirror coil actuation

The same results as shown for the NI calibration are given in the table 7 and in the figure 9.

At low frequency, the calibration with the pcal is within $5\% \pm 10 - 20\%$ from the main stream calibration.

GPS	F_i (Hz)	f_i (Hz)	Gain ($\mu\text{m}/\text{V}$)	Coherence	
				pcal	coil
879664070	19.0	18.0	11.2137 ± 0.4277	0.99490	0.98744
879664070	19.0	23.0	35.3291 ± 1.3286	0.99490	0.98846
879664070	24.0	23.0	23.7842 ± 1.5324	0.90888	0.98846
879664070	69.0	68.0	13.8682 ± 0.2990	0.99975	0.99974
879664070	119.0	118.0	13.4800 ± 0.3578	0.99791	0.99898
879664070	119.0	123.0	13.8030 ± 0.3650	0.99791	0.99903
879664070	254.0	253.0	12.6202 ± 0.5216	0.98590	0.99108
879664070	459.0	458.0	12.2440 ± 0.6411	0.95832	0.98875
879664397	459.0	458.0	12.4132 ± 0.7734	0.97948	0.98989
879664540	459.0	458.0	12.8569 ± 0.9200	0.97446	0.98787
879664650	459.0	458.0	12.5194 ± 0.5442	0.97964	0.99170
879664976	854.0	853.0	13.6753 ± 0.4551	0.99431	0.99593
879665307	1014.0	1013.0	14.8973 ± 0.5265	0.98538	0.99865
879665633	19.0	18.0	11.2103 ± 0.5367	0.99352	0.98854
879665633	19.0	23.0	35.2171 ± 1.6612	0.99352	0.98936
879665633	24.0	23.0	18.9806 ± 1.7208	0.88536	0.98936
879665633	69.0	68.0	13.7458 ± 0.3033	0.99985	0.99983
879665633	119.0	118.0	13.2942 ± 0.3876	0.99858	0.99895
879665633	119.0	123.0	13.8214 ± 0.4034	0.99858	0.99894
879665633	254.0	253.0	13.0460 ± 0.6433	0.99088	0.98961
879665633	459.0	458.0	12.4448 ± 0.8012	0.95951	0.99134

Table 4: **NI mirror coil actuation gain in LN mode**, measured using the NI pcal. All the datasets are given. The associated frequencies are given: the pcal lines at F_i and the coil actuation line at f_i . The last two columns give the coherence of the dark fringe to Ca_NI_ADC and Sc_NI_LoopIn respectively.

f_i (Hz)	Gain ($\mu\text{m}/\text{V}$)
18.0	11.212 ± 0.343
23.0	35.279 ± 1.064
68.0	13.807 ± 0.213
118.0	13.391 ± 0.264
123.0	13.812 ± 0.272
253.0	12.811 ± 0.414
458.0	12.478 ± 0.334
853.0	13.675 ± 0.455
1013.0	14.897 ± 0.526

Table 5: *Average NI mirror coil actuation gain in LN mode, computed using the NI pcal. The statistical errors are given.*

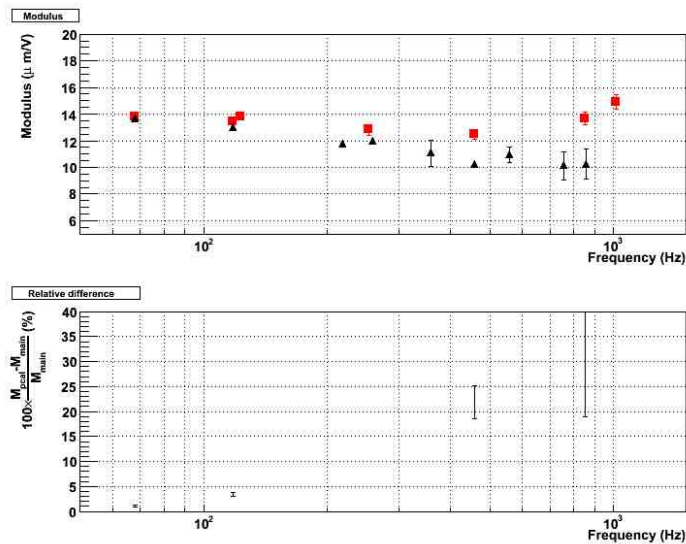


Figure 7: *Average NI mirror coil actuation gain in LN mode vs frequency computed using the NI pcal (red triangles). The statistical errors are shown. The coil actuation gain in LN mode computed from the main stream calibration is also shown as empty squares for comparison.*

f_i (Hz)	Gain ($\mu\text{m}/\text{V}$)
16.0	5.743 ± 0.251
21.0	23.727 ± 0.742
51.0	12.664 ± 0.240
116.0	13.231 ± 0.342
251.0	12.730 ± 0.423
456.0	12.408 ± 0.331
555.9	12.429 ± 0.258
701.0	12.816 ± 0.333
1011.0	15.064 ± 0.592

Table 6: *Average NE mirror coil actuation gain in LN mode, computed using the NI pcal. The statistical errors are given.*

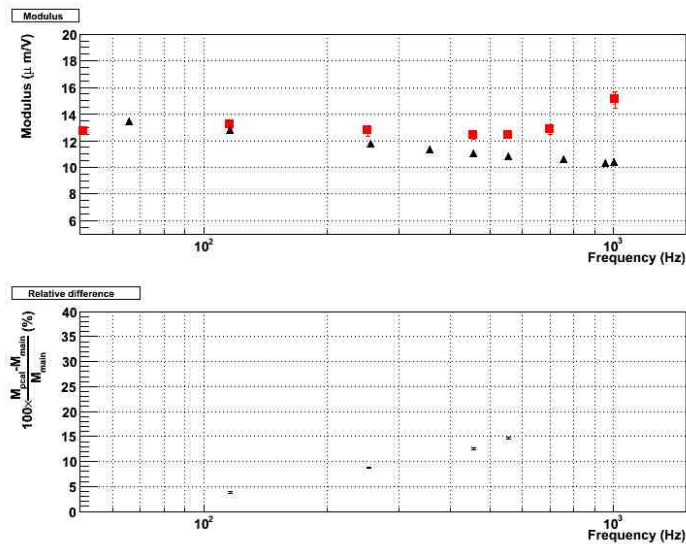


Figure 8: *Average NE mirror coil actuation gain in LN mode vs frequency computed using the NI pcal (red triangles). The statistical errors are shown. The coil actuation gain in LN mode computed from the main stream calibration is also shown as empty squares for comparison.*

f_i (Hz)	Gain ($\mu\text{m}/\text{V}$)
16.5	6.024 ± 0.462
21.5	23.210 ± 0.756
51.5	11.241 ± 0.216
116.5	11.463 ± 0.306
251.5	11.199 ± 0.395
456.5	10.981 ± 0.308
556.4	10.993 ± 0.247
701.5	11.443 ± 0.301
1011.5	13.439 ± 0.544

Table 7: *Average WE mirror coil actuation gain in LN mode, computed using the NI pcal. The statistical errors are given.*

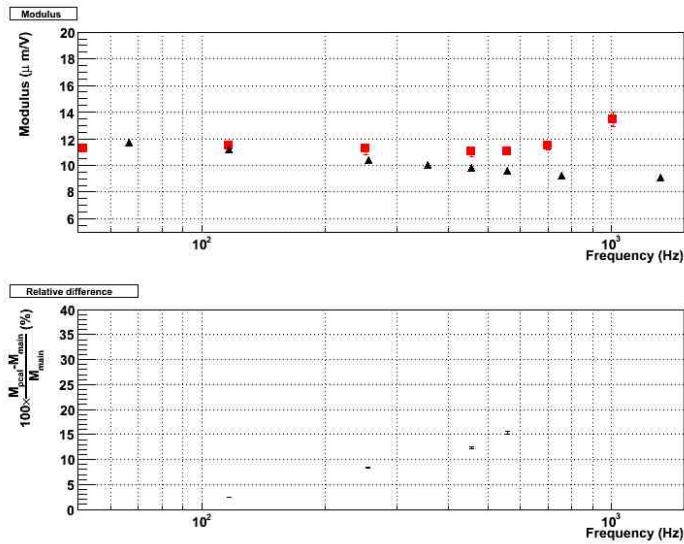


Figure 9: *Average WE mirror coil actuation gain in LN mode vs frequency computed using the NI pcal (red triangles). The statistical errors are shown. The coil actuation gain in LN mode computed from the main stream calibration is also shown as empty squares for comparison.*

6 Conclusions

The NI pcal was used during VSR1 to check the mirror actuation calibration obtained from the main stream calibration.

The setup of the NI pcal is such that a single laser beam hits the center of the NI mirror. A photodiode has been calibrated in order to estimate the power of the beam. The systematic errors of the power calibration are estimated to 10-20%.

With the pcal setup used during VSR1, the pcal laser beam is overlapped by the main ITF beam. The validity of the mirror actuation calibration with the pcal is thus limited up to a few 100's Hz since at high frequency the mirror deformation induced by the pcal beam has an amplitude higher than the mirror motion.

In the validity range of the analysis, $\sim 50 - 200$ Hz, the pcal calibration is in agreement with the main stream calibration within $\sim 5\%$. Taking into account the systematic errors of the pcal calibration, **the main stream calibration of the NI, NE and WE mirror actuation modulus is confirmed within 10-20% below 200 Hz.**

References

- [1] L. Rolland, F. Marion, B. Mours *Mirror and marionette actuation calibration for VSR1* (2008) VIR-015B-08.
- [2] O. Véziant, Thèse de l'Université de Savoie (2003)
- [3] S. Hild et al. **Class. Quantum Grav.** Vol.24, Issue 22, 5681-5688 (2007) (gr-qc0710.1229).